SindhUniv. Res. Jour. (Sci. Ser.) Vol. 50 (003) 371-378 (2018)

http://doi.org/10.26692/sujo/2018.09.0062

SINDH UNIVERSITY RESEARCH JOURNAL (SCIENCE SERIES)

Automated Extraction of Retinal Blood Vessels for Early Diagnosis of Diabetic Retinopathy Using Enhancement Filters and Adaboost

K. DAHRI++, S. A. KHOWAJA, G. LAGHARI*, S. NIZAMANI**, S.CHANDIO**

Institute of Information and Communication Technology, University of Sindh, Jamshoro, Pakistan

Received 01st July 2017 and Revised 17th April 2018

Abstract: This paper proposes an automated extraction and segmentation of blood vessels to diagnose the symptoms of diabetic retinopathy at early stage. The proposed method has been evaluated on two commonly used, publicly available benchmark datasets DRIVE, and STARE. The results show that the proposed method attains the best trade-off results in terms of effectiveness and efficiency and performs comparably better than state-of-the-art methods. The average accuracy on DRIVE, and STARE database turns out to be 0.973, and 0.952, respectively.

Keywords: Retinal vessel extraction, Feature Engineering, Image Enhancement, Ada Boost, Medical Imaging, Matched Filters.

1. INTRODUCTION

The vessel features, such as length, width, branching patterns, can provide a base to early diagnosis of pathologies caused by the changes in morphology of blood vessels (Mendonca 2006). The properties of the ocular fundus image such as fovea, optical disks, and mainly the blood vessels (vascular tree) can be affected by major diseases including diabetes, diabetic retinal pathology, hypertension, arteriosclerosis, choroidal neovascularization, and artery occlusion (Mendonca 2006). Retinal image is one of the sources by which these pathologies can be determined in accordance with the changes in retinal blood vessels. Thus, analysis on different parts of the eye can be performed via fundus image. This motivates researchers to work on the segmentation of retinal blood vessels for the early diagnosis of such diseases by accurately detecting the changes in retinal blood vessels. Retinal image is one of the source by which these pathologies can be determined in accordance with the changes in retinal blood vessels.

However, manual diagnosis of these pathologies from retinal images is very difficult, and sometimes impossible, due to the complex nature of vascular networks. Consequently, it requires an automated solution.

In this paper, we propose an automated extraction and segmentation of blood vessels from the fundus color image to diagnose the symptoms of diabetic retinopathy at early stage.

The main contributions of the paper are following:

- To enhance the fundus image for accurate extraction and segmentation of blood vessels by sophisticated preprocessing.
- To use only seven features for training the model making the model less complicated.
- To use a recently emerged classification algorithm AdaBoost, which extensively fine tunes the weak learners to make their impact significant.

To contextualize, we provide brief details on diabetic retinopathy in Section 2 and related literature in Section 3. In Section 4, we provide details on preprocessing, feature extraction, and classification steps in our proposed method. Section 5 provides details on how we evaluate our proposed method, which leads to results in Section 6. Finally, we arrive at the conclusion in Section 7.

2. DIABETIC RETINOPATHY

Diabetic retinopathy, caused by the complications of diabetes, is a leading cause of blindness in adults (Zhang, 2018).. Diabetic retinopathy can cause severe loss of vision and blindness owing to changes in retinal blood vessels. There are no early stage symptoms indicating diabetic retinopathy. However, as it develops it causes loss of vision and the recovery is not possible as shown in (**Fig. 1)**

Recent surveys carried out in Pakistan show that a significant number of diabetic patients have diabetic retinopathy also indicating that diabetic retinopathy is highly correlated with diabetes (Rahman *et al.*, 2011) (Shaikh, 2007) According to these reports, Pakistan is at 10th position having 6.5 million diabetic patients and it is estimated that Pakistan will be among top seven countries having most diabetic patients by 2030.

To diagnose diabetic retinopathy, hospitals in Pakistan mostly use two methods: Fundus Fluorescein Angiography and Optical Coherence Tomography. We briefly describe the two methods in this section.

++Corresponding Author: kamran.dahri@usindh.edu.pk

*Institute of Mathematics and Computer Science, University of Sindh, Jamshoro, Pakistan

**Department of Computer Science, Sindh University Campus Mirpurkhas, Pakistan

Fundus Fluorescein Angiography (FFA*)* test examines retina for different retinal conditions by injecting a special diagnostic dye which circulates through the retinal blood vessels (Nandakumar, *et al.,* 2012). To monitor the eye condition, photographs of retinal blood vessels are captured by specialized digital camera at different instances to observe any leakage, poor circulation, or blockage. (**Fig. 2**) illustrates FFA. FFA test procedure takes more than half an hour and it has the following side effects.

- Skin color may slightly change to yellow for next 24-48 hours.
- Very small number of patients may get allergic reaction after injecting the dye.
- Patients may get nausea or vomiting.

Optical Coherence Tomography (OCT) is a computerized imaging technique, which generates a 3D image of an eye using laser lights **(Fig. 3)** OCT rapidly acquires the images of eye by creating an array of light; these images represent the tissue layers within the retina (Liu, *et al.,*2011) OCT allows doctors to detect changes or abnormalities in the retina by dilating the pupil. A laser beam is directed into the eye to capture the structural images and scan the crucial areas of an eye. In OCT, nerve fiber layer thickness measurement can be affected by the signal strength. Thus, pupillary dilation is required to achieve the desired image quality. OCT procedure normally takes 5-10 minutes.

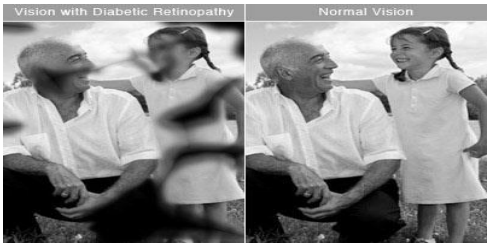

Fig. 1. Vision differences due to DR

2. RELATED WORK

Recent years have seen progress in the field of retinal vessel segmentation for detecting diabetic retinopathy. Vessel segmentation studies are mainly divided into two studies i.e. unsupervised and supervise methods.

Unsupervised algorithms use morphological, tracking, or filtering based methods. Vessel tracking performs segmentation from either manually defined initial set of points or tracking the centerline of the vessels. Such kind of vessel estimation profiles can be tracked using various methods such as multiscale profiles (Wink, *et al.,* 2004) Bayesian method (Yin, *et al.,* 2012) Gaussian (Li, *et al.,*2005) and generic parameters (Liang *et al.,*1994.) Morphological methods not only enhance the retinal images but also can be applied for vessel tree segmentation from the background (Bahadar *et al.,*2016) (Fang, *et al.,*2003) Filtering based techniques employ different kernels for enhancing and extracting blood vessels from retinal images, some of the methods using filtering techniques are COSFIRE (Azzopardi, *et al.,* 2015) Gabor (Soares, *et al.,* 2006) wavelet (Gang, *et al.,*2002) Gaussian, (Wang, *et al.,*2013) and matched filters (Gang, *et al.,* 2002) (Zhang, *et al.,*2010).

One of the most widely used methods for retinal vessel segmentation is the supervised method. This requires, for training, the ground truth images manually labeled by human experts (also referred to as the gold standard). Prominent features are computed based on either global or local image characteristics, to guide the training algorithm. Effective segmentation of the supervised methods is based on the combination of meaningful representation of features and the learning algorithm. The classification algorithms employed for such studies include adaptive boosting (AdaBoost) (Freund *et al.,*1997), support vector machines (Marín, *et al.,* 2011) artificial neural networks (Marín, *et al.,* 2011) and k-nearest neighbors . (Niemeijer *et al.,* 2004) proposed a combination of multiscale Gaussian filter based features with k-nearest neighbors algorithm to identify vessel and background pixels (Niemeijer *et al.,* 2004) presented a method based on multiscale Gabor filters for feature extraction and constructed a ridge detector using similar approach. computed 7-D features based on local intensities and moment-invariants and learnt the representations with feed-forward neural networks (Marín, *et al.,* 2011) (Fraz *et al.* 2012) extracted the features using Gabor filter responses, morphological characteristics, gradient vector field, and line strength measures with boosted trees as the classification algorithm to extract the vessels (Ricci *et al.,* 2007) proposed a support vector machines algorithm with local pixel intensities and rotational-invariant based features (Lupascu *et al.* 2010), used AdaBoost classifier with various feature extraction methods (i.e. 41 features) to obtain a good accuracy on the DRIVE dataset but with the trade-off for increased complexity. (Wang *et al.,* 2015) proposed convolutional neural networks for feature extraction combined with ensemble of classifiers using random forests to segment the retinal vessels. Their method is based on the creation of super pixels using simple linear iterative clustering method, which is the core basis for feature extraction method. You et al. utilized radial projections as their feature vector with support vector machines classifier in a semi-supervised manner. (Roychowdhury *et al.* 2014) computed 8 features using first and second order gradient images from the pixel neighborhood and

employed Gaussian mixture models as the learning algorithm. (Zhu *et al.* 2016) used extreme learning machines with the combination of different features (a total of 39) to extract the said vessels. (Zhu *et al.* 2016) extracted almost same number of features with classification and regression tress for classification of vessel and non-vessel pixels proposed method based on support vector machines with Gabor wavelet and multiscale filters . (Aslani *et al.* 2016) extracted 17 features using COSFIRE filters, multi-orientation and multiscale features with RF classification algorithm.

It is obvious that supervised learning requires demanding computational capability compared to unsupervised approaches. However, the results are far more accurate with former than the latter. Thus, we propose multi-level learning algorithm based on varying number of features to differentiate between vessel and non-vessel pixels

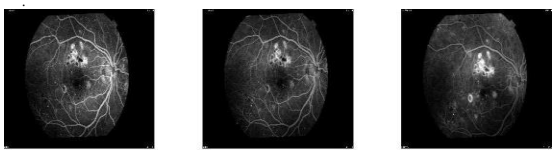

Fig. 2. Illustration of Fundus Fluorescein Angiography.

3. PROPOSED METHOD

We propose an automated way of blood vessel extraction and segmentation for retina by only capturing the fundus color image. To optimize, the key features include preprocessing with fundus image enhanced using the combination of contrast limited adaptive histogram equalization (CLAHE) and top-hat transformation, followed by the vessel map enhancement using Hessian based Frangi filters (Cf. Section 4.1), small set of features extracted from local intensities, Gabor filter and phase congruency concepts which are easy to compute and consume less time for their computation (Cf. Section 4.2), and finally, using adaptive boosting (AdaBoost) classification algorithm for training and classifying the vessel pixels. (**Fig. 4**) illustrates the overall process of our proposed method.

We first preprocess the fundus image. The resultant image will undergo the feature extraction stage where multiple features are extracted at each level. At each level, our AdaBoost model learns the extracted features and the final results are combined using majority voting based decision level fusion.

Like previous studies we also consider the green channel of the RGB image as it shows the highest contrast against the background and consider the pixels inside the field of view (FOV) region. There are also two main reasons not to choose the pixels outside of FOV region. First, they are considered to be the background pixels. Second, there is no known medical application for this.

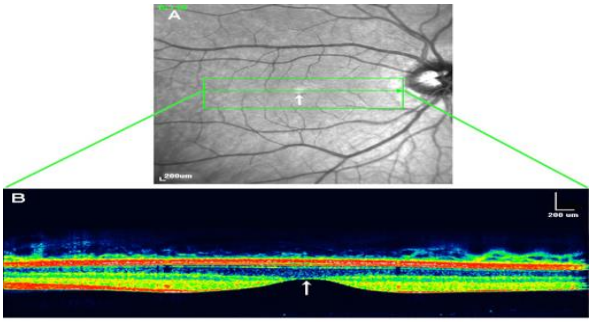

Fig. 3 OCT result of Macula/Fovea

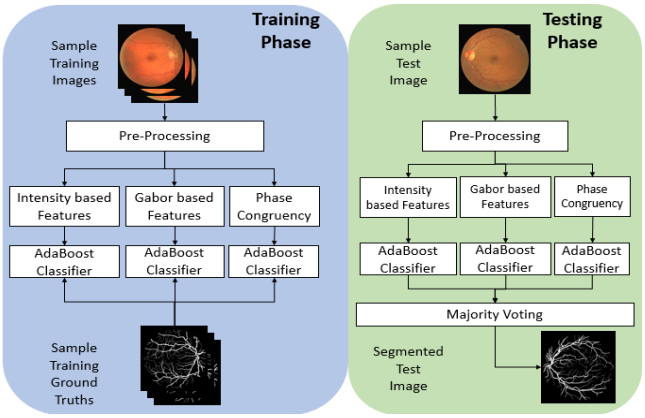

Fig.4 Steps in proposed method

Pre-Processing We use preprocessing step to enhance the images with respect to contrast and in homogeneity. We extract the FOV in compliance with the fundus image and extract the vessel using the feature engineering and data-driven techniques. To keep the major and prominent blood vessels, we further enhance the vessel map using image erosion.

(Fig 5) illustrates our proposed preprocessing stage for fundus image and vessel enhancement. First, we apply 5x5 median filter on the extracted green channel image to reduce image noise while preserving the edge information. Second, we smooth the filtered image and extract the FOV region from the image. The smoothing of image is important otherwise the vessels around the edges of the image are mistakenly detected as possible vessels—the false positives. To ensure that no false vessel is detected at the boundaries of FOV region, we also apply the method proposed by Azzopardi *et al.* (2015) We apply CIElab color space for thresholding the luminance to extract the FOV region image.

It is necessary to overcome the homogeneity issue for segmenting the blood vessels accurately. In this regard, we apply contrast limited adaptive histogram equalization (CLAHE) algorithm, which improves the contrast in the local regions keeping the noise constant in the homogeneous regions. (Han, *et al.*, 2014) To

further reduce the noise, we employ morphological top-hat transformation. This transformation completes the process of enhancing the image.

Finally, we apply Frangi filter to enhance the vessel map. Existing methods have proved that Frangi filter requires less computation time yet efficiently enhances the vessel profile for segmentation (Bankhead, *et al.*, 2012). The vertical and horizontal diagonals for the Hessian matrix using Frangi filter are computed using second-order derivatives of the image and is defined in (**equation 1).**

$$I(x) = \max_{\sigma} I(x, \sigma) \quad (1)$$

Where x refers to the pixel, I represent the filter, and σ is the standard deviation of the Gaussian derivative. The Hessian matrix is shown in (**equation 2)**

$$H = \begin{pmatrix} H_{xx} & H_{xy} \\ H_{yx} & H_{yy} \end{pmatrix} \quad (2)$$

Where each of the elements in the matrix represents the direction of second-order partial derivative. Hessian matrix takes into account the Eigen values to determine the probability of pixel x being the vessel. These Eigen values are denoted by λ_1 and λ_2, respectively. The notation of these variables is defined in (**equation 3)**

$$|\lambda_1| \leq |\lambda_2| > 0 \; and \; I(x, \sigma) = 0 \quad (3)$$

Based on the above equations and notations, the Frangi filter using Hessian matrix is defined in (**equation 4)**

$$I(x) = \begin{cases} e^{\left(-\frac{L_b^2}{2\gamma^2}\right)}\left(1 - e^{\left(\frac{R^2}{2\alpha^2}\right)}\right), & if\ \lambda_2 \leq 0 \\ 0, & otherwise \end{cases} \quad (4)$$

Where $L_b = \frac{|\lambda_1|}{|\lambda_2|}$, $R = \sqrt{\lambda_1^2 + \lambda_2^2}$ (5)

The blob-like structures are differentiated from linear structures using L_b and γ, while noise and vessels are differentiated using R and α. The values of the controlling parameters γ, α, *and* σ are empirically determined to be 0.8, 12, and {1,1.1, … ,4} respectively. The result of the preprocessing stage on retinal fundus image is shown in (**Fig 6)**

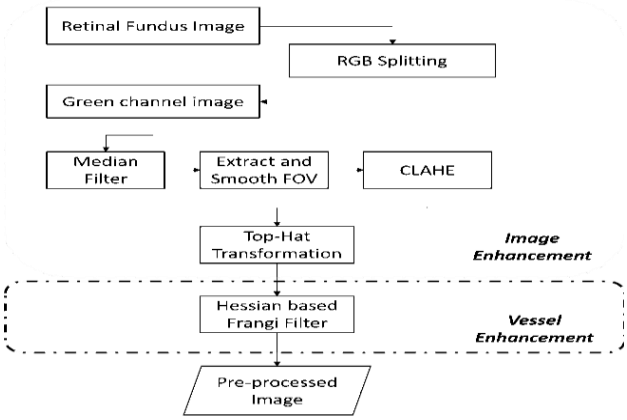

Fig. 5. Proposed preprocessing for retinal fundus image

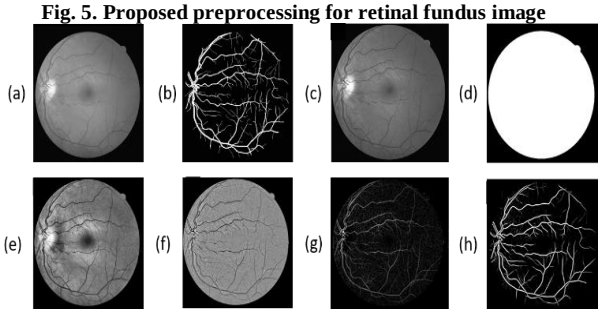

Fig. 6. Effect of preprocessing stage on retinal fundus image (a) original image (b) ground truth image (c) green channel image (d) mask (e) contrast enhancement (f) background subtracted image (g) morphological transformation (h) preprocessed image using Hessian based Frangi filter.

Feature Extraction The extracted features are crucial for the effectiveness of the supervised methods, as they help easily distinguish vessel pixels from non-vessel pixels. Many existing studies have employed intensity-based features. However these features alone cannot extract the vessels accurately. Nonetheless, the use of intensity-based features cannot be ruled out disregarded as they provide essential information regarding the distribution of intensities inside the image. Previous studies have used feature level based fusion method for combining different kinds of features. In this study, we use decision level fusion i.e. the majority voting from the result of each classifier. We define the details of each set of features in following subsections.

Intensity Based Features: We use the sliding window to extract the intensity-based features. These features are derived from the histograms of the preprocessed image. These features are defined in (**equations 6–9)**

$$feat_1 = \frac{1}{m^2}\sum_{(x,y)\epsilon[1:m]^2} I_{x,y} \quad (6)$$

$$feat_2 = \frac{1}{m^2}\sum_{(x,y)\epsilon[1:m]^2}\left(I_{x,y} - feat_1\right)^2 \quad (7)$$

$$feat_3 = \frac{1}{m^2}\sum_{(x,y)\epsilon[1:m]^2}\left(I_{x,y} - feat_1\right)^3 \quad (8)$$

$$feat_4 = \frac{1}{m^2}\sum_{(x,y)\epsilon[1:m]^2}\left(I_{x,y} - feat_1\right)^4 \quad (9)$$

Where m represents the size *and* x, y are coordinates of the image I. The features defined in (**equations 6–9)** are referred to as mean (first moment), variance (second moment), skewness (third moment), and kurtosis (fourth moment), respectively

*Gabor Filter Based Features:*These features relate to the characteristics of the texture. Varying Gaussian kernels using 2-D convolution are applied to compute such features. The varying kernels are centered on abscissa with respect to the Cartesian coordinates having orientation φ. With these notations Gabor filter kernel denoted by $K_{\varphi,\sigma,\rho,\lambda,\theta}$ is defined in (**equation 10)**

$$K_{\varphi,\sigma,\rho,\lambda,\theta}(i,j) = \exp\left(-\frac{i^2+\rho^2 j^2}{2\sigma^2}\right) cos\left(2\pi\frac{i}{\lambda}+\theta\right) (10)$$

The Gaussian module can be modified using the spatial aspect ratio ρ and deviation σ, which define the shape of the Gaussian kernel. Whereas the sinusoid module is characterized by a phase offset θ, and wavelength λ. The size of the pixel in the Gabor kernel is expressed as (v_i, v_j) that defines the change of scale using the orientation φ, and translation of the kernel to the center by (x_c, y_c) as shown in (**equation 11)**

$$K_{\varphi,\sigma,\rho,\lambda,\theta}(x,y) = \exp\left(-\frac{i'^2+\rho^2 j'^2}{2\sigma^2}\right) cos\left(2\pi\frac{i'}{\lambda}+\theta\right) (11)$$

Where:

$$i' = (x-x_c)v_i cos\varphi + (y-y_c)v_j sin\varphi \quad (12)$$

$$j' = (x-x_c)v_i sin\varphi + (y-y_c)v_j cos\varphi \quad (13)$$

The ellipsoidal envelope of the Gabor kernel is controlled by the position, size, and orientation of the parallel stripes having different weights. The variable λ is used for scaling the stripes by modifying the wavelength, while keeping the dimension and the orientation constant. As the wavelength is influenced by the image borders, less than the fifth of image dimension is considered. The orientation φ determines the angle of the parallel stripes, hence we can rotate or orient at the specific position by modifying φ. The kernel symmetry is determined by the offset part θ, suggesting that the kernel is asymmetric if $\theta = \frac{\pi}{4}$, and symmetric if $\theta = 0$. The aspect ratio ρ determines the ellipticity. For the Gaussian deviation σ, we replace it with the bandwidth b, as suggested by Glatard et al.. The Gabor features are computed by convolving with filter banks defined in (**equation 14)**

$$R(i,j) = g(i,j) * I(i,j) \sum_{p=0}^{P=1} \sum_{q=0}^{Q} g(p,q) \cdot I(i-p, j-q) \quad (14)$$

The convolution operation is denoted by "*". P and Q represent the size of the filter mask. The absolute mean deviation values from the filtered image are computed to derive the local squared energy from window size of $N_x N_y$ and mean μ **(equation 15)** Similarly, the amplitude of the local responses is defined in (**equation 16)**

$$feat_5 = SE(i,j) = \left(\frac{1}{N}\sum_{(a,b)\epsilon\omega} |R(a,b) - \mu|\right)^2 (15)$$

$$feat_6 = Amp(i,j) = |R(i,j)| \quad (16)$$

*Phase Congruency:*The use of phase congruency brings a significant advantage in terms of feature representation since it takes into consideration the line and step edges of those pixels where the maximal phase of the Fourier components is recorded. It provides the feature points with an absolute measure and is invariant to illumination problems in images. To compute the overall phase congruency of the fundus image, we employ the method proposed by Kovesi **(equation 17)**

$$.feat_7 = PH(i,j) = \frac{\sum_\varphi \sum_s w_\varphi(i,j)\lfloor A_{s,\varphi}\Delta\Phi_{s,\varphi}(i,j) - \eta_\varphi \rfloor}{\sum_\varphi \sum_s A_{s,\varphi}(i,j) + \xi} \quad (17)$$

Where s and φ refer to the scale and orientation from 0 to π, respectively. The (i,j) are coordinates of the image and η is the noise response and is determined to be 2.96 in our study, ξ is a constant value 0.00001 to avoid the division by zero in case of the local energy of fundus image getting very small. A denotes the angular rotation and is defined as $A = \left\{E | 0 \le E \le \pi, E mod \left(\frac{\pi}{12}\right) = 0\right\}$ with respect to the structuring element defined and $\lfloor x \rfloor$ is defined as $\lfloor x \rfloor = \begin{cases} x, & if\ x \ge 0 \\ 0, if\ x < 0 \end{cases}$. The weight for the phase congruency where the narrow spread of filter response is recorded is defined by w_φ. The said weighting function is constituted as shown in **(equation 18)** using a sigmoid function.

$$w_\varphi(i,j) = \frac{1}{1+e^{\vartheta(C-\Upsilon(i,j))}} \quad (18)$$

We penalize the spreading of the phase congruency values from the filter responses using variable C, which is a constant set to be 0.37. The gain value is defined as ϑ and is set to be 9.65 to control the sharpness of C. The spread $\Upsilon(i,j)$ is computed as shown in **(equation 19)**

$$\Upsilon(i,j) = \frac{1}{K}\left(\frac{\sum_k A_k(i.j)}{A_{max}(i,j)+\xi}\right) \quad (19)$$

Where K is the number of scales, $A_k(i,j)$ is the filter response amplitude, and $A_{max}(i,j)$ is the maximum amplitude at point (i,j).

Classification In our proposed method, we employ the AdaBoost algorithm introduced by Freund and Schapire. This algorithm has recently gained a lot of attention in the field of computer vision, specifically in medical imaging due to its simple implementation and fast speed. It can be used with different base classifiers as learners. AdaBoost extensively fine tunes the weak learners to make their impact significant and finally uses all the fine-tuned weak learners in an ensemble manner. The computation of the AdaBoost classifier is given in **(equation 20)**

$$H(x) = sign\left(\sum_{p=1}^{P} \omega_p h_p(x)\right) \quad (20)$$

Where ω_p refers to the corresponding weights for the training instances x and $H(x)$ and $h_p(x)$ refer to the strong classifier, weak classifiers respectively.

Evaluation

In this section, we describe how we evaluate our proposed approach.

Evaluation MetricWe evaluate the performance of the proposed method using three widely used evaluation metrics: sensitivity, specificity, and accuracy. The metrics are defined in equations 21–23 respectively.

$$Senstivity\ (S_e) = \frac{TP}{TP+FN} \quad (21)$$

$$Specificity\ (S_p) = \frac{TN}{TN+FP} \quad (22)$$

$$Accuracy\ (A_c) = \frac{TP+TN}{TP+FP+TN+FN} \quad (23)$$

Where:

- TP = pixel correctly identified as vessel
- FP = pixel falsely identified as vessel
- TN = pixel correctly identified as non-vessel
- FN = pixel falsely identified as non-vessel

DatasetTo run our analysis for retinal vessel segmentation using the proposed method, we use two datasets: Digital Retinal Images for Vessel Extraction (DRIVE) [3], and Structures Analysis of the Retina (STARE) [4]. These datasets are also used in the studies against which we compare our results.

The DRIVE dataset comprises 40 JPEG images, of which 33 do not show any sign of diabetic retinopathy while 7 show signs of mild early diabetic retinopathy. The images were acquired with a 45° field of view (FOV). Each image was captured using 8 bits per color plane at 768 x 584 pixels and accompanies a corresponding FOV mask image.

The STARE dataset comprises 20 images with half of images indicating no sign of diabetic retinopathy. While, half of the images are indicated with obscured or confused appearance of the blood vessel in varying portions of the image. The images were captured at 35° FOV. Each image has 24 bits per pixel and size of 605x700 pixels. There are no FOV masks available, however, we generated these in an automated manner.

The ground truth for the fund us images is used from the first observer for both the datasets.

PlatformWe have implemented our method in MATLAB. We run our analysis in MATLAB R2015b using an Intel Core i7 with 8GB RAM and 3.3 GHz CPU.

4. RESULTS

As we used different feature extraction methods, first we compare the individual feature sets. Table 1 shows the result for individual feature set in terms of sensitivity, specificity, and accuracy for the DRIVE dataset. Here we observe that in terms of sensitivity, Gabor Filter Based Feature with Energy is the best while Phase Congruency Based Feature is the worst. For specificity, all the features compare almost equally, yet Phase Congruency Based Feature stands out. Similarly, for the overall performance with respect to accuracy Gabor Filter Based Feature with Energy is relatively better.

Next, we compare the effectiveness of our proposed method with state of the art. Table 2 shows the results for DRIVE and STARE datasets. It is apparent that our proposed method performs better than many existing approaches and is at par with the methods by Wang and Han respectively.

Table 1. Performance comparison of individual feature sets

Feature Set	S_e	S_p	A_c
LIBF	0.7862	0.9427	0.9189
$GFBF_{Amp}$	0.8569	0.9596	0.9437
$GFBF_{Eng}$	0.8576	0.9614	0.9462
PCBF	0.5897	0.9754	0.9384

LIBF: Local Intensities Based Features, $GFBF_{Amp}$: Gabor Filter Based Feature with Mean Amplitude, $GFBF_{Eng}$: Gabor Filter Based Feature with Energy, PCBF: Phase Congruency Based Feature.

Moreover, our proposed method is amongst the top performers for the STARE dataset and shows fine trade-offs on accuracy and less computational complexity.

Finally, we evaluate the efficiency of the approach. Table 3 reports the average segmentation time. Here also our proposed method takes less time.To conclude, our proposed method with just 7-D features has low complexity yet it strikes the right balance between effectiveness in terms of accuracy and efficiency in terms of average segmentation time and is equally comparable with existing methods. The qualitative results for some of the retinal images are also shown in (**Fig 7**)

Table 2.Comparison of effectiveness of our proposed method with state-of-the-art methods.

Method	Drive			Stare		
	Se	Sp	Acc	Se	Sp	Acc
[3]	-	-	0.944	-	-	0.952
[16]	0.733	0.978	0.946	0.721	0.975	0.948
[26]	0.720	-	0.960	-	-	-
[22]	0.707	0.980	0.945	0.694	0.982	0.953
[24]	0.741	0.981	0.948	0.755	0.976	0.953
[42]	0.725	0.980	0.947	0.781	0.984	0.963
[33]	0.754	0.980	0.951	0.756	0.984	0.960
[43]	0.677	0.987	0.977	0.810	0.979	0.981
[27]	0.817	0.973	0.977	0.810	0.979	0.981
[44]	0.641	0.963	0.935	0.616	0.962	0.935
[45]	0.765	0.979	0.961	0.612	0.979	0.941

PM†	**0.883**	**0.989**	**0.973**	**0.819**	**0.980**	**0.952**

† Proposed Method.

Table 3.Comparison of efficiency of our proposed method with state-of-the-art methods.

Method	Time† (seconds)
[16]	18.70
[46]	15.00
[22]	90.00
[24]	120.00
[3]	900.00
Proposed Method	**12.16**

†Average processing time per image

5. CONCLUSION

In this paper, we proposed a retinal vessel segmentation method. Retinal vessel segmentation is considered to be the primary step for detection of diabetic retinopathy. Our method is based on vessel enhancement and 7-D features using AdaBoost algorithm. The image enhancement is performed using CLAHE method followed by top-hat transformation for enhancing the retinal image. Then, vessel map is enhanced using Hessian based Frangi filters. In this study, we extracted three kinds of features namely, local intensity-based, Gabor filter based, and phase congruency based features. We found that for the DRIVE dataset, Gabor

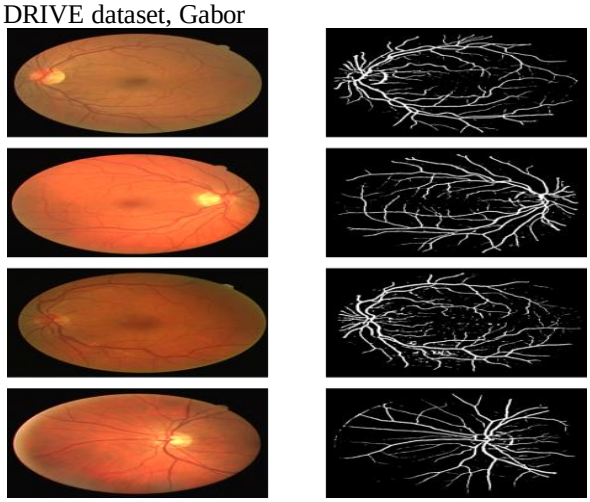

Fig. 7 Qualitative results for vessel extraction.

Filter Based Feature with Energy is the best on sensitivity metric, while Phase Congruency Based Feature produces better results for specificity metric. Likewise, Gabor Filter Based Feature with Energy is relatively better for accuracy metric.Furthermore, we see that our proposed method, which only using seven features, compared to state of the art performs better. It produces good segmentation result with the best trade-off in terms of effectiveness (accuracy) and efficiency (computational complexity) for vessel segmentation

5. ACKNOWLEDGEMENT

We acknowledge Dr. Khalid Iqbal Talpur for his moral support and Liaquat National Eye Hospital, for providing necessary information and valuable suggestions for improving the readability of this paper.

REFERENCES:

Aslani S. and H. Sarnel, (2016) "A new supervised retinal vessel segmentation method based on robust hybrid features," *Biomed. Signal Process. Control*, vol. 30, 1–12.

Azzopardi, G., N. Strisciuglio, M. Vento, and N. Petkov, (2015) "Trainable COSFIRE filters for vessel delineation with application to retinal images," *Med. Image Anal.*, vol. 19, no. 1, 46–57.

Abramoff, M. D. (2004) "Comparative study of retinal vessel segmentation methods on a new publicly available database," in *SPIE Medical Imaging*, 648–656.

Bahadar K., A. A Khaliq, and M. Shahid, (2016) "A Morphological Hessian Based Approach for Retinal Blood Vessels Segmentation and Denoising Using Region Based Otsu Thresholding," *PLoS One*, vol. 11, no. 7, p. e0158996.

Bankhead, P., C. N. Scholfield, J. G. McGeown, and T. M. Curtis, (2012) "Fast Retinal Vessel Detection and Measurement Using Wavelets and Edge Location Refinement," *PLoS One*, vol. 7, no. 3, p. e32435

Cheng, E., L. Du, Y. Wu, V. Megalooikonomou and H. Ling, (2014) Discriminative vessel segmentation in retinal images by fusing context-aware hybrid features," *Mach. Vis. Appl.*, vol. 25, no. 7, 1779–1792.

Frangi, A. F., W. J. Niessen, K. L. Vincken, and M. A. Viergever, (1998) "Multiscale vessel enhancement filtering," in *Medical Image Computing and Computer-Assisted Intervention*, 130–137.

Fang, B., W. Hsu and M. L. Lee, (2003) "Reconstruction of vascular structures in retinal images," in *International Conference on Image Processing (Cat. No.03CH37429)*, vol. 3, 157-60.

Freund Y. and R. E. Schapire, (1997) "A Decision-Theoretic Generalization of On-Line Learning and an Application to Boosting," *J. Comput. Syst. Sci.*, vol. 55, no. 1, 119–139.

Glatard, T., J. Montagnat, and I. E. Magnin, (2004) "Texture based medical image indexing and retrieval," in *Proceedings of the 6th ACM SIGMM international workshop on Multimedia information retrieval - MIR '04*, 135Pp.

Gang, L., and S. M. Krishnan, (2002) "Detection and measurement of retinal vessels in fundus images using amplitude modified second-order Gaussian filter," *IEEE Trans. Biomed. Eng.*, vol. 49, no. 2, 168–172.

Han, Z., Y. Yin, X. Meng, G. Yang, and X. Yan, (2014) "Blood Vessel Segmentation in Pathological Retinal Image," in *2014 IEEE International Conference on Data Mining Workshop*, 960–967.

Hoover, A. D., V. Kouznetsova, M. Goldbaum, (2000) "Locating blood vessels in retinal images by piecewise threshold probing of a matched filter response," *IEEE Trans. Med. Imaging*, vol. 19, no. 3, , 203–210.

Liu, T., A. Y. Hu, A. Kaines, F. Yu, S. D. Schwartz, and J.-P. Hubschman, (2011) "A Pilot Study Of Normative Data For Macular Thickness and Volume Measurements Using Cirrus High-Definition Optical Coherence Tomography," *Retina*, vol. 31, no. 9, 1944–1950.

Li, H., W. Hsu, M. L. Lee, and T. Y. Wong, (2005) "Automatic Grading of Retinal Vessel Caliber," *IEEE Trans. Biomed. Eng.*, vol. 52, no. 7, 1352–1355.

Liang Z., M. S. Rzeszotarski, L. J. Singerman, and J. M. Chokreff, (1994.) "The detection and quantification of retinopathy using digital angiograms," *IEEE Trans. Med. Imaging*, vol. 13, no. 4, 619–626,

Lupascu, C. A., D. Tegolo, and E. Trucco, (2010) "FABC: Retinal Vessel Segmentation Using AdaBoost," *IEEE Trans. Inf. Technol. Biomed.*, vol. 14, no. 5, 1267–1274.

Mendonca A. M. and A. Campilho, (2006) "Segmentation of retinal blood vessels by combining the detection of centerlines and morphological reconstruction," *IEEE Trans. Med. Imaging*, vol. 25, no. 9, 1200–1213.

Marín, D., A. Aquino, M. E. Gegundez-Arias, and J. M. Bravo, (2011) "A New Supervised Method for Blood Vessel Segmentation in Retinal Images by Using Gray-Level and Moment Invariants-Based Features," *IEEE Trans. Med. Imaging*, vol. 30, no. 1,146–158.

Niemeijer, M., J. Staal, B. van Ginneken, M. Loog, and Fraz M. M. (2012) "An Ensemble Classification-Based Approach Applied to Retinal Blood Vessel Segmentation," *IEEE Trans. Biomed. Eng.*, vol. 59, no. 9, 2538–2548

Nandakumar, N., S. Buzney, and J. J. Weiter, (2012) "Lipofuscin and the Principles of Fundus Autofluorescence: A Review," *Semin. Ophthalmol.*, vol. 27, no. 5–6, 197–201.

Rahman, S., R. Nawaz, G. J. Khan, and A. H. Aamir, (2011) "Frequency of Diabetic Retinopathy in Hypertensive Diabetic Patients in a Tertiary Care Hospital of Peshawar, Pakistan," *J. Ayub Med. Coll.*, vol. 23, no. 2, 133–135.

Roychowdhury, S., D. Koozekanani, and K. Parhi, (2014) "Blood Vessel Segmentation of Fundus Images by Major Vessel Extraction and Sub-Image Classification," *IEEE J. Biomed. Heal. Informatics*, vol. 19, no. 3, 1118–1128.

Ricci E. and R. Perfetti, (2007) "Retinal Blood Vessel Segmentation Using Line Operators and Support Vector Classification," *IEEE Trans. Med. Imaging*, vol. 26, no. 10, 1357–1365.

Shaikh, A. M. (2007) "Diabetic Retinopathy: Analyzing the Pakistan survey and Evaluating local resources," *Community Eye Heal.*, vol. 20, no. 61Pp.

Soares, J. V. B., J. J. G. Leandro, R. M. Cesar, H. F. Jelinek, and M. J. Cree, (2006) "Retinal vessel segmentation using the 2-D Gabor wavelet and supervised classification," *IEEE Trans. Med. Imaging*, vol. 25, no. 9, 1214–1222.

Setiawan, A. W., T. R. Mengko, O. S. Santoso, and A. B. Suksmono, (2013) "Color retinal image enhancement using CLAHE," in *International Conference on ICT for Smart Society*, 1–3.

Tang, S., T. Lin, J. Yang, J. Fan, D. Ai, and Y. Wang, (2015) "Retinal Vessel Segmentation Using Supervised Classification Based on Multi-Scale Vessel Filtering and Gabor Wavelet," *J. Med. Imaging Heal. Informatics*, vol. 5, no. 7, 1571–1574.

Wink, O., W. J. Niessen, and M. A. Viergever, (2004) "Multiscale Vessel Tracking," *IEEE Trans. Med. Imaging*, vol. 23, no. 1, 130–133.

Wang, Y., G. Ji, P. Lin, and E. Trucco, (2013) "Retinal vessel segmentation using multiwavelet kernels and multiscale hierarchical decomposition," *Pattern Recognit.* vol. 46, no. 8, 2117–2133.

Wang, S., Y. Yin, G. Cao, B. Wei, Y. Zheng, and G. Yang, (2015) "Hierarchical retinal blood vessel segmentation based on feature and ensemble learning," *Neurocomputing*, vol. 149, 708–717.

You, X., Q. Peng, Y. Yuan, Y. Cheung, and J. Lei, (2011) "Segmentation of retinal blood vessels using the radial projection and semi-supervised approach," *Pattern Recognit.*, vol. 44, no. 2314–2324.

Zhang, B., L. Zhang, L. Zhang, and F. Karray, (2010) "Retinal vessel extraction by matched filter with first-order derivative of Gaussian," *Comput. Biol. Med.*, vol. 40, no. 4, 438–445.

Yin, Y., M. Adel, and S. Bourennane, (2012) "Retinal vessel segmentation using a probabilistic tracking method," *Pattern Recognit.*, vol. 45, no. 4, 1235–1244, .

Zou, B., J. Cui, C. Zhu, Y. Xiang, and H. Wu, (2016) "An Ensemble Retinal Vessel Segmentation Based on Supervised Learning in Fundus Images," *Chinese J.*

Electron., vol. 25, no. 3, 503–511.

Zhang, X. (2018). “Prevalence of Diabetic Retinopathy in the United States, 2005–2008.” *JAMA : the journal of the American Medical Association* 304.6 649–656.